Supporting Information

Spatially aromatic fences of metal-organic frameworks for manipulating the electron spin of fulleropyrrolidine nitroxide radical

Jiamei Cao[a,c], Yongqiang Feng[*,a], Shengju Zhou[a,c], Xiaofeng Sun[a,c], Taishan Wang[b], Chunru Wang[b], and Hongguang Li[*,a]

[a] *State Key Laboratory of Solid Lubrication & Laboratory of Clean Energy Chemistry and Materials, Lanzhou Institute of Chemical Physics, Chinese Academy of Sciences, Lanzhou, 730000, China. Email: fengyq@licp.cas.cn; hgli@licp.cas.cn.*
[b] *Beijing National Laboratory for Molecular Sciences, Laboratory of Molecular Nanostructure and Nanotechnology, Institute of Chemistry, Chinese Academy of Sciences, Beijing 100190, China.*
[c] *University of Chinese Academy of Sciences, Beijing, 100049, China*

Contents

Experimental Section:

Materials

Zinc nitrate hexahydrate (> 98%), aluminium nitrate nonahydrate (> 98%), N,N-diethylformamide (DEF, > 99%), 4',4'',4''' -benzene-1,3,5-triyl-tri-benzoic acid (H_3BTB, > 97%), and 1,4-benzenedicarboxylic acid (DBC, > 99%) were purchased from J&K. 4-Amino-4-carboxy-2,2,6,6-tetramethylpiperidine-1-oxyl (TOAC) was purchased from Acros, fullerene (C_{60}) was obtained from Suzhou Dade Carbon Nanotechnology Co. Ltd. Toluene (A. R.) was purified by distilled in vacuum and dried over 4A molecular sieve. All the other compounds were used as received.

Methods

General Information: Field-emission scanning electron microscope (FESEM; JEOL-7600F) was used to examine the morphology of the samples. Thermogravimetric analysis (TGA) was performed with a temperature rate of 5 ℃ min^{-1} under air flow using a SHIMADZU TA instrument DTG-60H apparatus. Crystal structures of the sample were examined by a Shimadzu XRD-7000 diffractometer with Cu K radiation (λ = 1.54056 Å). Fourier transform-infrared spectroscopy (FT-IR) was carried out on a VERTEX-70/70v spectrometer (Bruker Optics, Germany). Nitrogen adsorption/desorption isotherm was measured by a Quantachrome Autosorb AS-1 instrument at 77 K. Matrix-assisted laser desorption/ionization time-of-flight mass spectrum (MALDI-TOF-MS) were performed on a BRUKER Autoflex III instrument. Continuous-wave electron spin resonance (ESR) spectra were recorded on JEOL FA200 instrument with X band.

Synthesis of MOF-177

The crystal of MOF-177 was synthesized by solvothermal method as previously reported[1,2]. 80 mg of $Zn(NO_3)_2 \cdot 6H_2O$ and 20 mg of H_3BTB were dissolved in 1 mL of DEF, and then the solution was sealed into a glass vial, heated at a rate of 2 ℃ min^{-1} to 100 ℃ and held for 23 h, and cooled at a rate of 0.2 ℃ min^{-1} to room temperature. The morphology of the as-prepared crystals was shown in Figure S1.

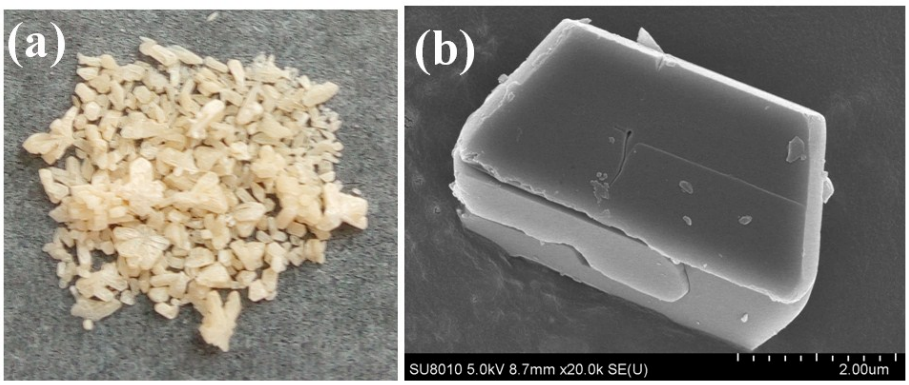

Figure S1. (a) Optical and (b) SEM images of as-synthesized MOF-177.

TGA and Elemental Analysis of MOF-177

The as-synthesized crystaline MOF-177 was dried at 100 ℃. TGA experiment was performed in air with a temperature rate of 5 ℃ min^{-1} using a SHIMADZU TA instrument DTG-60H apparatus. The first weight loss (30.65%) appeared below 200 ℃ belongs to departure of the guest molecule DEF and H_2O, and the second corresponds to deformation of the MOF skeleton, see Figure S2. Elemental test revealed a weight ratio as C 54.27%, N 4.42%, H 5.20%. Combined with the TG results we can conclude the formula of the prepared MOF-177 as $ZnO_4(BTB)_2 \cdot (DEF)_3 \cdot (H_2O)_9$.

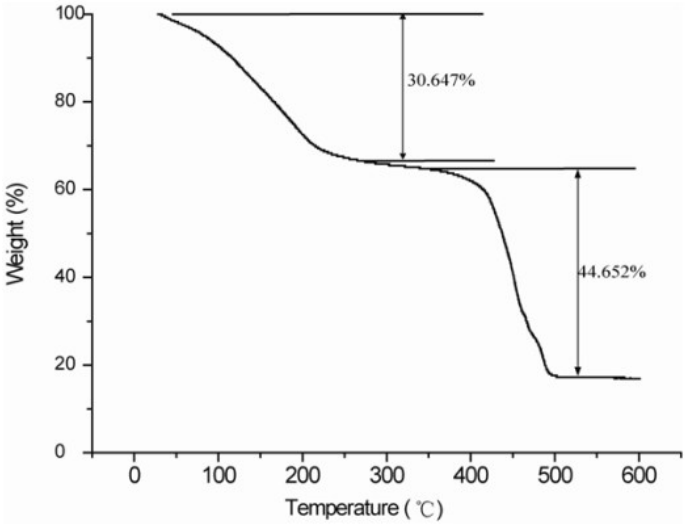

Figure S2. TGA profile of MOF-177 measured with a temperature rate of 5 ℃ min^{-1} in the range of 20~600 ℃.

Synthesis of MIL-53

The crystal of MIL-53 was synthesized by heating a mixture of $Al(NO_3)_3 \cdot 9H_2O$ (3.8995 g), BDC (0.8643 g) and deionized water (15 mL) in a Teflon vial sealed in a stainless steel tank at 220 ℃ for three days.[3] Figure S3 show the photographic and SEM images of the as-synthesized crystal.

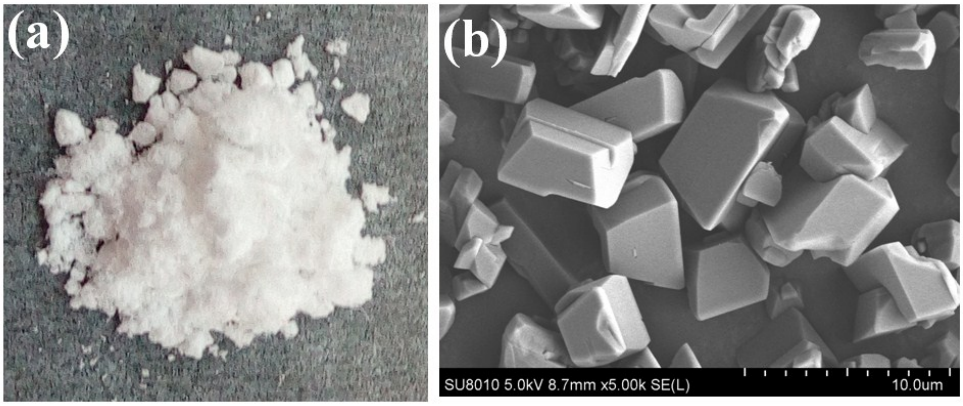

Figure S3. (a) Optical and (b) SEM images of as-synthesized MIL-53.

TGA and Elemental Analysis of MIL-53

The TGA analysis of the as-synthesized crystaline MIL-53 was performed in air with a temperature rate of 5 ℃ min^{-1} using a SHIMADZU TA instrument DTG-60H apparatus. As shown in Figure S4, the first two-step weight loss (ca. 37%) below 420 ℃ belongs to departure of the guest molecule DBC in the channels of MIL-53, and the second weight loss from 420~610 ℃ corresponds to elimination of the DBC linker. Above 610 ℃ the crystal collapsed to Al_2O_3. Elemental test revealed a weight ratio as C 50.55%, H 2.83%. Combined with the TG results we can conclude the formula of the prepared MIL-53 as $Al(OH)[O_2CC_6H_4CO_2]\cdot[HO_2CC_6H_4CO_2H]_{0.70}$.

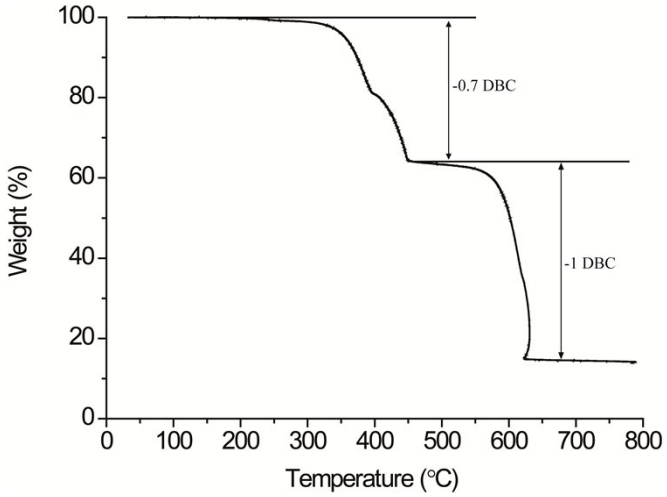

Figure S4. TGA profile of MIL-53 measured with a temperature rate of 5 ℃ min^{-1} in the range of 20~800 ℃.

PXRD Measurement for MIL-53

Varied-temperature PXRD measurement of the as-synthesized MIL-53 crystals was carried out at a temperature range of 25~800 ℃ as shown in Figure S5. It can be seen clearly that the XRD pattern retained unchanged below

300 ℃, then an intermidiate phase appeared between 400~600 ℃. Finally the sample turned to Al_2O_3 above 600 ℃,[3] which was in good agreement with the TGA result.

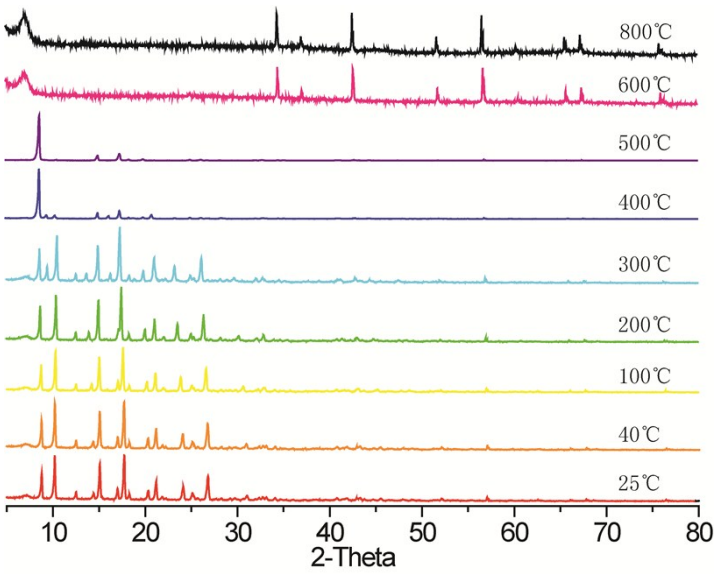

Figure S5. Varied-temperature XRD profiles of MIL-53 measured with a temperature rate of 5 ℃ min^{-1} in the range of 25~800 ℃

Synthesis and Characterization of Fulleropyrrolidine, 3,4-fulleropyrrolidine-2-spiro-4′-(2′,2′,6′,6′-tetramethylpiperidine-1′-oxyl, (1)

The spin-active fulleropyrrolidine **1** was synthesized according to the literatures with some modification.[4,5] To a stirred solution containing 300 mg of C_{60} in 250 mL of toluene added 100 mg of TOAC and 80 mg of paraformaldehyde. The mixture solution was refluxed under argon atmosphere for 1 h monitored by TLC. After cooling, the solution was condensed by a rotating vacuum evaporator, and the target product was isolated by flash silicon column chromatography using toluene as eluent. Figure S6 was the mass spectrum of **1** showing a molecular mass of 904[$M+H^+$], 888[$M-CH_3$] and 873[$M-2CH_3$].

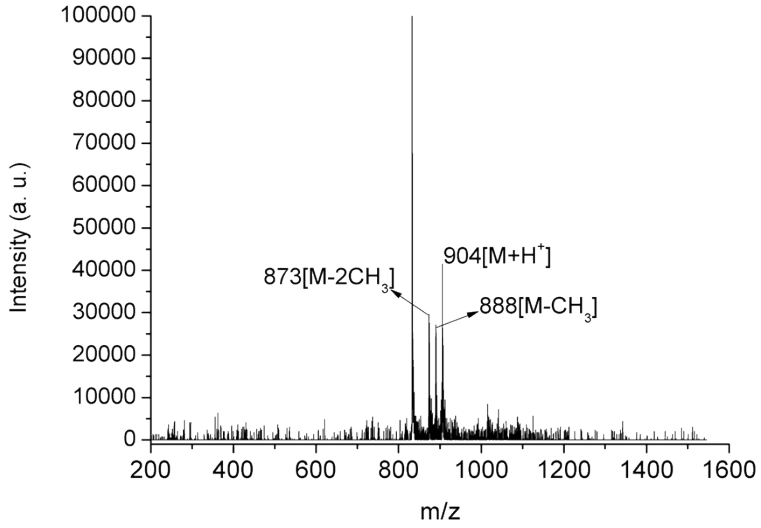

Figure S6. MALDI-TOF-MS profile of **1**.

The ESR spectrum of **1** was recorded on a JEOL FA200 system. The ESR pattern of **1** in toluene at room temperature shows three lines with a intensity ratio of 1:1:1 (Figure S7). It can be seen that the solution state ESR spectrum exhibited completely isotropic characteristics with a set of spin parameters of a_{iso} = 15.10 G, g = 2.0080.

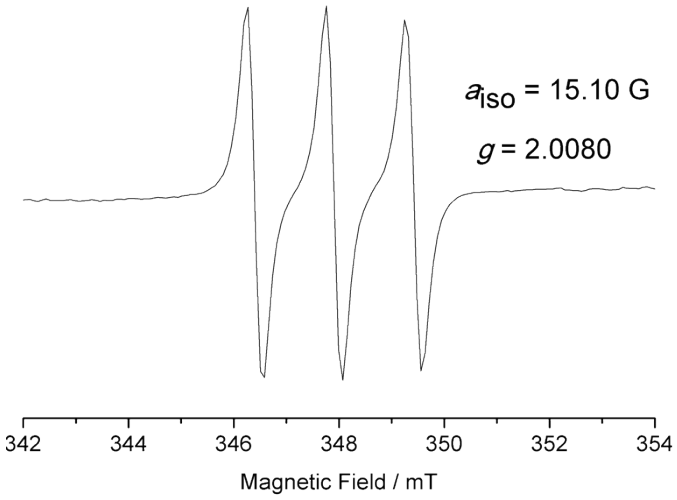

Figure S7. ESR spectra of **1** in toluene at room temperature (a_{iso} = 15.10 G, g = 2.0080).

Preparation of 1@MOF-177, 1@MIL-53, 1/MOF-177 and 1/MIL-53

For the preparation of **1**@MOF-177 and **1**@MIL-53, firstly the as-synthesized crystal samples (denoted as MOF-177(as) and MIL-53(as)) were activated to expel the solvent molecules encapsulated in the pores of MOF-177 and MIL-53. The crystal sample of MOF-177(as)/MIL-53(as) was separately immersed in dichloromethane (DCM) for three days and the solvent was refreshed for every 24 h. Then the crystals (denoted as MOF-177(act) and MIL-53(act)) was filtered, washed by fresh toluene three times and dried under N_2. Secondly, 5 mg of

activated MOF-177(act)/MIL-53(act) crystals were immersed into a toluene solution of **1** with a concentration of *ca*. 1 mg mL^{-1} for several days to let **1** enter the MOF pores completely. After the supernatant was decanted, the obtained complex was washed with fresh toluene several times until no ESR signal was detected and dried under a N_2 flow. The procedure for the preparation of **1**/MOF-177 and **1**/MIL-53 was similar to their corresponding counterpart except that MOF-177(as) and MIL-53(as) without any activation were used. In these cases, the guest molecule **1** was unable to freely enter into the pores of MOF-177 and MIL-53, instead it may tamely tend to mainly absorbed on the surface of the crystals.

XRD Measurement

PXRD measurement was then performed at room temperature. For both case in MOF-177 and MIL-53, DCM activation caused a phase alternation due to the lattice perturbation by the guest molecules. However, the crystal matrix maintained intact, which make sure the ability to encapsulate fullerene molecules. It can be seen clearly from Figure S8a that around the diffraction angle of 6° emerged a bilateral peak in **1**@MOF-177, corresponding to a lattice distance of about 14 Å, which can be ascribed to the incarceration of **1** into the pores of MOF-177.[6,7] Whereas in the case of **1**@MIL-53, the XRD peak intensity of the first two reflexes (2θ = 8.59, 10.04, respectively) decreased remarkably after a swarm of guest molecules were in residence, which was attributed to the probably saturated pore filling of MIL-53 by **1**.[8,9]

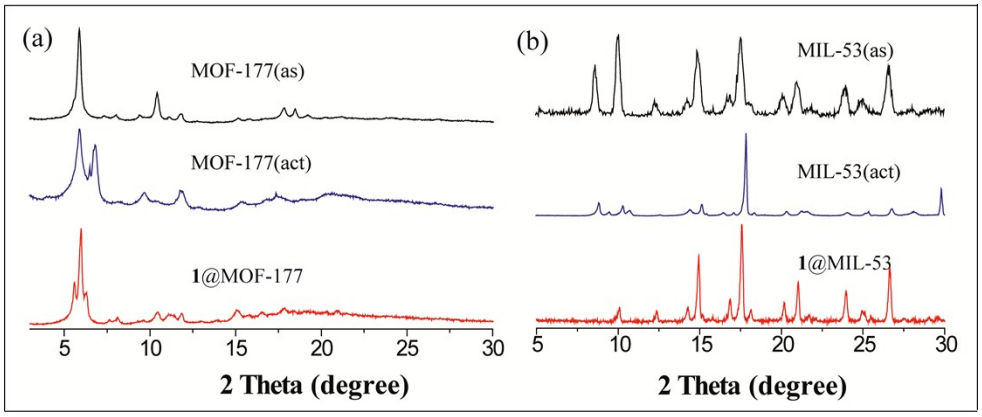

Figure S8. PXRD spectra of (a) MOF-177(as), MOF-177(act), **1**@MOF-177 and (b) MIL-53(as), MIL-53(act), **1**@MIL-53.

EDS Measurement

EDS experiment was conducted through a field-emission scanning electron microscope (FESEM; JEOL-7600F) instrument. As can be seen from Figure S9a, the as-synthesized sample MOF-177(as) contains a N content with a mass ratio of 4.23%, which was derived from the solvent molecule DEF used in the solvothermal process. After DCM activation, the N element was absent in MOF-177(act), indicating that the DEF molecules involved in the

pores of MOF-177 were completely squeezed out. Therefore, the N content observed in **1**@MOF-177 was definitely originated from the guest **1**, which confirmed the encapsulation of **1** into the pores of MOF-177. Whereas for MIL-53(as), no N element was detected in that there was no nitrogen source available during the synthesis. After the DCM activation, the BDC molecules incarcerated in the channels of MIL-53(as) was excluded out, and then the fullerene molecule **1** consequently entered into the 1D channel of MIL-53(act).

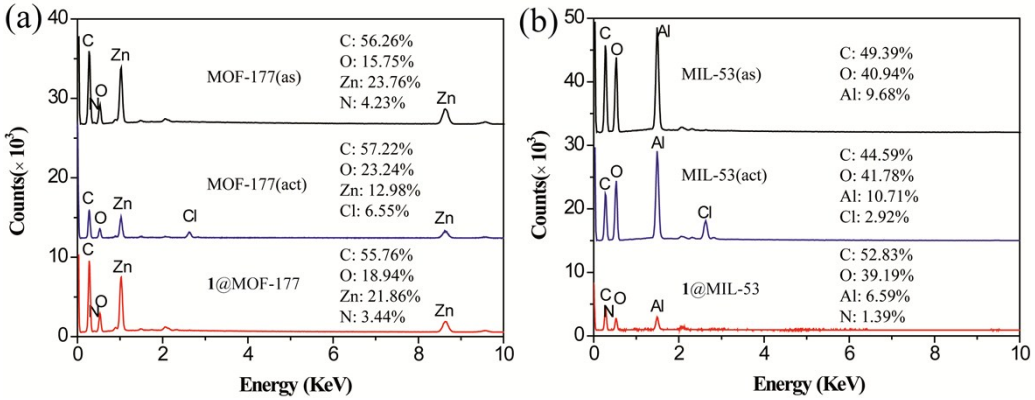

Figure S9. EDS spectra of (a) MOF-177(as), MOF-177(act), **1**@MOF-177 and (b) MIL-53(as), MIL-53(act), **1**@MIL-53.

TG Analysis

Figure S10 showed the TG profiles of these six samples measured with a temperature rate of 5 ℃ min^{-1} under an air flow. In MOF-177(as), it was apparent that there exist two weight loss steps below 200 ℃ corresponding to the evaporation of DEF and BTB in the pores of MOF-177. After DCM activation, the slope of the weight loss curve became gentle. When the guest molecule was exchanged by fullerene **1**, the plateau stage in **1**@MOF-177 shifted forward to 120 ℃. In contrast, the two-step weight loss in MIL-53(as) below 400 ℃ corresponding to 0.7 DBC molecule encaged in the channel of MIL-53 turned to a single step after DCM activation and fullerene exchange.

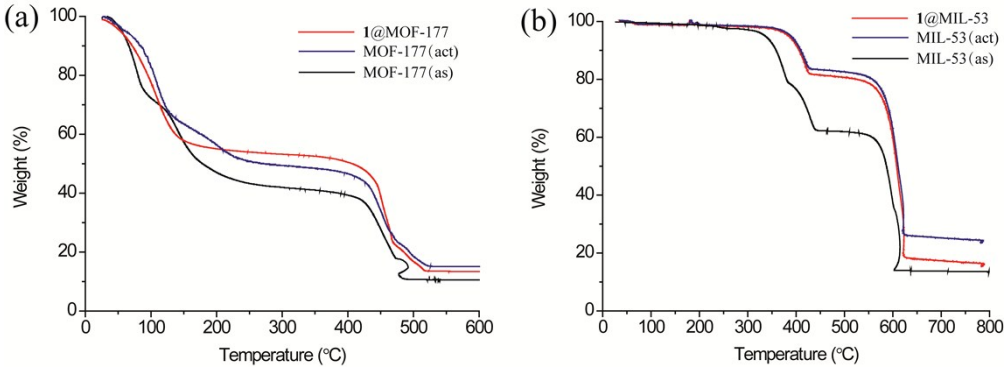

Figure S10. TG profiles of (a) MOF-177(as), MOF-177(act), **1**@MOF-177 and (b) MIL-53(as), MIL-53(act), **1**@MIL-53.

Fourier Transform Infrared (FTIR) Analysis

FTIR spectroscopy of the six samples was performed in a spectra range of 400~4000 cm^{-1} as shown in Figure S11. In the case of MOF-177, the absorption located at 1659 and 1537 cm^{-1} in MOF-177(as) were assigned to the asymmetric vibrational strenchings of –COO group connected to the ZnO_4 tetrahedron. It can be seen from Figure S7a that the peak intensity of these two bands changed and the position shifted to 1660 and 1543 cm^{-1} in MOF-177(act), and 1667 and 1551 cm^{-1}, respectively, in **1**@MOF-177 along with the guest exchange. Whereas for MIL-53, the asymmetric vibrational strenchings of –COO group connected to Al atom located at 1508 and 1600 cm^{-1} in MIL-53(as)[3] were enhanced greatly when the fullerene molecule was encapsulated.

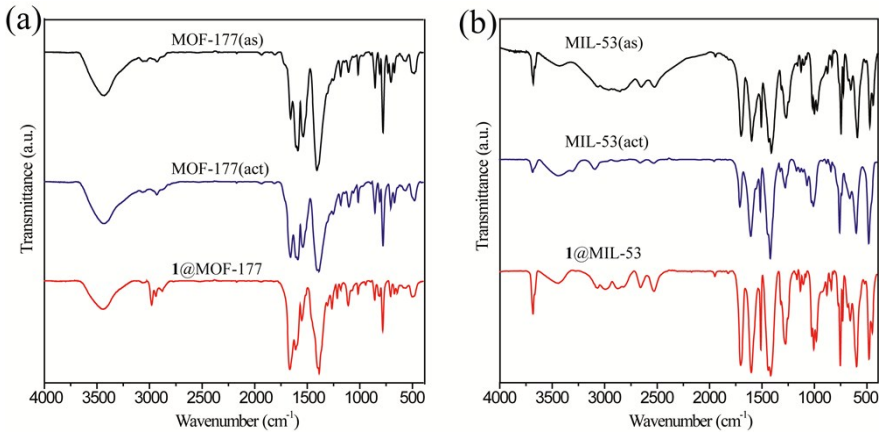

Figure S11. FTIR spectra of (a) MOF-177(as), MOF-177(act), **1**@MOF-177 and (b) MIL-53(as), MIL-53(act), **1**@MIL-53.

BET and Pore Volume Analysis of 1@MOF-177 and 1@MIL-53

Nitrogen adsorption/desorption isotherm was measured by a Quantachrome Autosorb AS-1 instrument at 77 K. About 100 mg of **1**@MOF-177/**1**@MIL-53 was dried at 60 ℃ for 12 h and then degased at 80 ℃ under vacuum for 24 h. Figure S12 show the nitrogen adsorption/desorption curves of **1**@MOF-177 and **1**@MIL-53. It can be seen that the BET surface area of **1**@MOF-177 retained as large as 3872.54 $m^2\ g^{-1}$, meanwhile the pore volume reached 4.384 $cm^3\ g^{-1}$ by BJH method; whereas for **1**@MIL-53, the BET surface area and pore volume were determined to be 139.30 $m^2\ g^{-1}$ and 0.194 $cm^3\ g^{-1}$ respectively, indicating that **1** were aggregated into the crowded 1D channels of MIL-53, but in MOF-177 they were probably mono-dispersed.

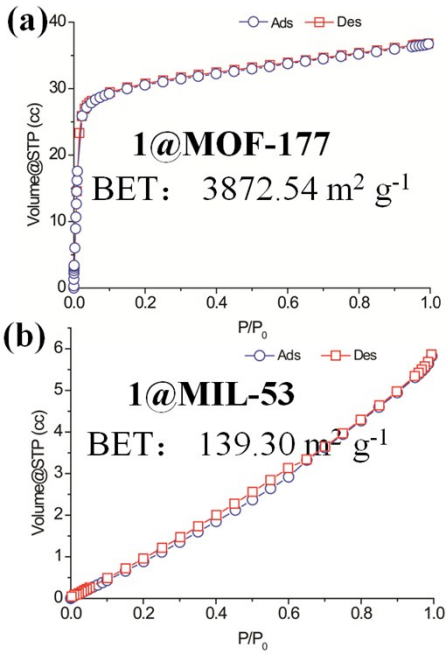

Figure S12. N_2 absorption (blue circle)/desorption (red square) curves of (a) **1**@MOF-177 and (b) **1**@MIL-53 at 77 K.

Varied-Temperature ESR Spectra of 1 in Solution State

The solution-state ESR spectra of **1** in toluene were recorded in the temperature range of 293~113 K as shown in Figure S13. At 293 K, three equivalent ESR lines derived from the coupling between the unpaired electron and the N atom with a nuclear spin of I (^{14}N) = 1 in fulleropyrrolidine radical **1** was observed. With the temperature decrease, the ESR pattern changed dramatically and the peak intensity in the low magnetic field enhanced at 213 K. Such paramagnetic anisotropy was resulted from the insufficient rotational averaging in resonance structure.[10] Below 213 K, the solution was frozen and the line width of the ESR spectra enlarged significantly due to the fast spin-lattice interaction. Finally at 113 K, the ESR pattern of **1** in solid solution was identical to that in MOF-177 and MIL-53 matrix, indicative of a restricted motion of **1** in frozen media and solid MOF matrix. Notably, in toluene solution the spin-active fullerene molecule **1** was disordered, whereas in MOF-177 and MIL-53 **1** was packed orderly.

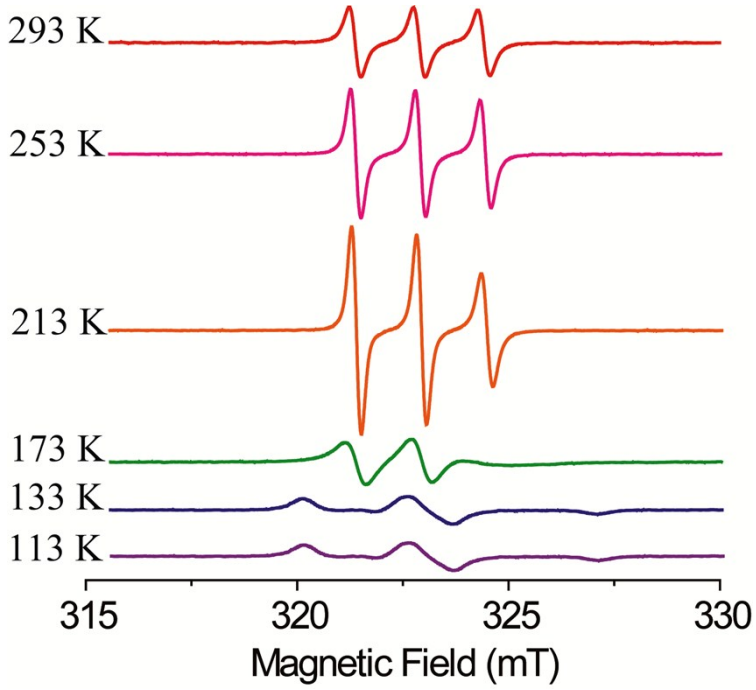

Figure S13. ESR profiles of **1** in toluene solution at varied temperatures.

Theoretical Section:

The simulation of the EPR spectra were carried out by the EasySpin package on the Matlab platform,[11,12] and the structural optimization of **1** was accomplished by using the Dmol3 code[13,14] with the generalized gradient approximation (GGA) functional of Perdew, Burke, and Ernzerhof (PBE)[15]. For closed- and open-shell systems, the spin-restricted and spin-unrestricted algorithms were used, respectively. All-electron double-numerical basis set with polarization functions (DNP) was applied for all atoms. To take into account relativistic effects, the all-electron scalar relativistic method utilizing the Douglas-Kroll-Hess (DKH) Hamiltonian[16,17], which is the most accurate approach available in DMol3 package, was chosen.

References in Supporting Information:

1 H. K. Chae, D. Y. Siberio-Pérez, J. Kim, Y. Go, M. Eddaoudi, A. J. Matzger, M. O'Keeffe and O. M. Yaghi, *Nature* **2004**, *427*, 523.

2 T. Loiseau, C. Serre, C. Huguenard, G. Fink, F. Taulelle, M. Henry, T. Bataille and G. Férey, *Chem. Eur. J.*, 2004, **10**, 1373-1382.

3 Y. Feng, T. Wang, Y. Li, J. Li, J. Wu, B. Wu, L. Jiang and C. Wang, *J. Am. Chem. Soc.*, 2015, **137**, 15055-15060.

4 F. Arena, F. Bullo, F. Conti, C. Corvaja, M. Maggini, M. Prato and G. Scorrano, *J. Am. Chem. Soc.*, 1997, **119**, 789-795.

5 C. Corvaja, M. Maggini, M. Prato, G. Scorrano and M. Venzin, *J. Am. Chem. Soc.*, 1995, **117**, 8857-8858.

6 Y. Feng, T. Wang, Y. Li, J. Li, J. Wu, B. Wu, L. Jiang and C. Wang, *J. Am. Chem. Soc.*, 2015, **137**, 15055-15060.

7 H. K. Chae, D. Y. Siberio-Perez, J. Kim, Y. Go, M. Eddaoudi, A. J. Matzger, M. O'Keeffe and O. M. Yaghi, *Nature*, 2004, **427**, 523-527.

8 T. Loiseau, C. Serre, C. Huguenard, G. Fink, F. Taulelle, M. Henry, T. Bataille and G. Férey, *Chem. Eur. J.*, 2004, **10**, 1373-1382.

9 A. M. Sheveleva, D. I. Kolokolov, A. A. Gabrienko, A. G. Stepanov, S. A. Gromilov, I. K. Shundrina, R. Z. Sagdeev, M. V. Fedin and E. G. Bagryanskaya, *J. Phys. Chem. Lett.*, 2014, **5**, 20-24.

10 Y. Ma, T. Wang, J. Y. Wu, Y. Feng, L. Jiang, C. Y. Shu and C. R. Wang, *Chem. Commun.*, 2012, **48**, 1 1570–11572.

11 S. Stoll and A. Schweiger, *J. Magn. Reson.*, 2006, **178**, 42-55.

12 S. Stoll and A. Schweiger, *Chem. Phys. Lett.*, 2003, **380**, 464-470.

13 B. Delley, *J. Chem. Phys.* **1990**, *92*, 508.

14 B. Delley, *J. Chem. Phys.* **2000**, *113*, 7756.

15 J. P. Perdew, K. Burke, M. Ernzerhof, *Phys. Rev. Lett.* **1996**, *77*, 3865.

16 M. Douglas, N. M. Kroll, *Ann. Phys.* **1974**, *82*, 89.

17 D. D. Koelling, B. N. Harmon, *J. Phys. C*: *Solid State Phys.* **1977**, *10*, 3107.